copy Ad

Directional spreading in surfbeat

A first assessment

Report submitted to RIKZ

Ad Reniers and Ap van Dongeren

TU Delft

Delft University of Technology

Section Fluid Mechanics

Contents

List of Figures

This progress report refers to part of the work done within the framework of the Dutch Center for Coastal Research (NCK). The primary objective of our research is to develop knowledge and methods for the prediction of the hydrodynamic conditions for the Dutch coast taking into account the morphodynamic behaviour in the nearshore zone.

In general the progress reports describe results, developments and new ideas obtained during our research. Most results have a preliminary status and should not be used without prior consent of the authors. The various topics described in the progress reports are brought together to gain more insight in the process to reach the primary objective. More detailed analyses of the various topics are or will be given in the form of journal papers. In addition attention is given to the (potential) links with work done by others.

1 Introduction

In the following we consider the forcing of long waves by normally or obliquely incident grouped short waves, also known as surf beat. Two mechanisms responsible for the generation of long waves are considered: the release of the bound long waves associated with changes in the spatial variation of the incident short wave energy [Longuet-Higgins and Stewart, 1964] and the time-varying position of the break point [Symonds et al., 1982]. These mechanisms are examined using linear shallow water equations on an alongshore uniform coast, with special attention for the cases of resonant interaction between the incident short waves and edge waves. The effect of directional spreading will be examined in detail. The reason to use linearized equations is twofold. First it renders the possibility to examine the various long wave generation mechanisms separately (without nonlinear interactions complicating the analysis). Second, it provides a quick assessment (computational time is an order of magnitude smaller) of the conditions which are interesting (such as edge waves) and can thus provide the necessary boundary conditions for the more complex nonlinear modelling.

2 Model equations

2.1 Wave transformation

In the following we consider processes which occur on the time scale of wave groups, which are typically in the order of thirty seconds to a few minutes. To obtain the appropriate equations the relevant variables are averaged over a single short wave period, i.e. short-wave averaged. Considering a non-stationary wave field of obliquely incident random waves on a variable bathymetry uniform in the alongshore direction, the balance for the short-wave averaged wave energy, E_w, is given by:

$$\frac{\partial E_w}{\partial t} + \frac{\partial E_w c_g \cos(\alpha)}{\partial x} = -S \tag{1}$$

where c_g represents the group velocity, S the wave energy dissipation, x the distance along the shore normal (positive onshore) and α the angle of incidence with respect the x-axis. To model the wave energy dissipation due to wave breaking the dissipation model according to Roelvink (1993) is introduced:

$$S = 2\alpha_d f_p (1 - e^{-\left(\frac{H_{rms}}{\gamma h}\right)^n}) E_w \tag{2}$$

where α_d, n and γ are the breaker parameters and f_p the peak frequency and H_{rms} the root mean square wave height. For values of n ¿ 100 the dissipation formulation corresponds to monochromatic wave breaking whereas n-values ¡ 20 are typically used to approximate wave dissipation in a random wave field.

The group velocity is obtained from linear wave theory:

$$c_g = \frac{d\omega_s}{dk_s} = \left(\frac{1}{2} + \frac{k_s h}{\sinh(2k_s h)}\right) c \tag{3}$$

where ω_s is the angular frequency of the short waves, k_s the wave number, h the total water depth (including set-up) and c the phase speed given by:

$$c = \frac{\omega_p}{k_s} \tag{4}$$

Given the water depth the wave number, k_s, can be obtained from the linear wave dispersion relation:

$$\omega_p{}^2 = g k_s \tanh(k_s h) \tag{5}$$

g being the gravitational acceleration. The wave incidence angle, α, is obtained from Snell's law:

$$\frac{\sin(\alpha)}{c} = \frac{\sin(\alpha_0)}{c_0} \tag{6}$$

where the subscript, 0, denotes a reference point offshore.

2.2 Long wave equations

The short-wave and depth-averaged linearized continuity equation is given by:

$$\frac{\partial \bar{\eta}}{\partial t} + \frac{\partial (du)}{\partial x} + \frac{\partial (dv)}{\partial y} = 0 \tag{7}$$

where d is the water depth without set-up. The cross-shore momentum balance reduces to:

$$\rho d \frac{\partial u}{\partial t} + \rho g d \frac{\partial \bar{\eta}}{\partial x} = -\frac{\partial S_{xx}}{\partial x} - \frac{\partial S_{xy}}{\partial y} \tag{8}$$

and the alongshore momentum equation:

$$\rho d \frac{\partial v}{\partial t} + \rho g d \frac{\partial \bar{\eta}}{\partial y} = -\frac{\partial S_{yy}}{\partial y} - \frac{\partial S_{yx}}{\partial x} \tag{9}$$

where the bottom shear stress and viscosity effects have been neglected. Combining these equations results in a single equation for the long wave surface elevation:

$$\frac{-1}{g}\frac{\partial^2 \bar{\eta}}{\partial t^2} + d\frac{\partial^2 \bar{\eta}}{\partial x^2} + \frac{\mathrm{d}d}{\mathrm{d}x}\frac{\partial \bar{\eta}}{\partial x} + \frac{\partial^2 \bar{\eta}}{\partial y^2} = \frac{1}{\rho g}\left(\frac{\partial^2 S_{xx}}{\partial x^2} + \frac{\partial 2 S_{yx}}{\partial x \partial y} + \frac{\partial^2 S_{yy}}{\partial y^2}\right) \tag{10}$$

In the field the forcing on the right hand side is governed by the frequency-directional spectrum of the short waves. Considering the full short wave spectrum, each combination of two primary waves of different frequency will result in a bichromatic wave train with an accompanying bound wave. In the following we therefore consider a combination of two short waves with different angular frequency, ω_i, and possibly different directions α_i. The long wave angular frequency is then given by:

$$\omega = \omega_1 - \omega_2 \tag{11}$$

and corresponding alongshore wave number:

$$k_y = k_1 \cdot \sin(\alpha_1) - k_2 \cdot \sin(\alpha_2) \tag{12}$$

respectively the cross-shore wave number of the long wave:

$$k_x = k_1 \cdot \cos(\alpha_1) - k_2 \cdot \cos(\alpha_2) \tag{13}$$

where k_i represents the wave number of the short waves.

Analogous to Schäffer [1990] we assume the long wave motions to be periodical in both time and alongshore direction:

$$\bar{\eta}(x,y,t) = \frac{1}{2}\hat{\eta}(x)exp[i(\omega t - k_y y)] + * \tag{14}$$

where $*$ stands for the complex conjugate, k_y represent the alongshore wave number of the long waves and ω is the long wave frequency. A similar assumption for the forcing induced by the radiation stress gradients gives:

$$S_{ij}(x,y,t) = s_{ij}(x)\left(\frac{1}{2}E(x)exp[i(\omega t - k_y y)]\right) + * \tag{15}$$

where:

$$s_{xx}(x) = \left(\frac{c_g}{c}\left(1+\cos^2\alpha\right) - \frac{1}{2}\right) \tag{16}$$

$$s_{xy}(x) = \left(\frac{c_g}{c}\cos\alpha\sin\alpha\right) \tag{17}$$

$$s_{yy}(x) = \left(\frac{c_g}{c}\left(1+\sin^2\alpha\right) - \frac{1}{2}\right) \tag{18}$$

and the energy modulation associated with the bichromatic wave grouping is given by:

$$E(x) = \hat{E}exp[-i\int k_x \mathrm{d}x] \tag{19}$$

where $\hat{E}$ represents the amplitude of the energy modulation. Introducing this into eq. 10 yields:

$$\left(\frac{\omega^2\hat{\eta}}{g} + d\frac{\mathrm{d}^2\hat{\eta}}{\mathrm{d}x^2} + \frac{\mathrm{d}d}{\mathrm{d}x}\frac{\mathrm{d}\hat{\eta}}{\mathrm{d}x} - k_y^2 d\hat{\eta}\right) exp[i(\omega t - k_y y)] + * = \tag{20}$$

$$\left(\frac{-1}{\rho g}\left(\frac{\mathrm{d}^2 s_{xx}E}{\mathrm{d}x^2} - 2ik_y\frac{\mathrm{d}s_{xy}E}{\mathrm{d}x} - k_y^2 s_{yy}E\right)\right) exp[i(\omega t - k_y y)] + *$$

This equation has been solved numerically using finite differences to yield the long wave surface elevation under obliquely incident wave groups, where the boundary conditions are given by a zero flux at the shore line and a weakly reflective boundary condition offshore taking into account the incident bound long wave associated with

the wave groups and free oblique outgoing long waves. On a horizontal plane the bound long wave elevation,η_b, can be obtained from eq. 20:

$$\left(\frac{\omega^2\hat{\eta}_b}{g} - {k_x}^2 d\hat{\eta}_b - k_y^2 d\hat{\eta}_b\right) exp[i(\omega t - k_y y)] + * = \tag{21}$$

$$\left(\frac{-1}{\rho g}\left(-{k_x}^2 s_{xx}\hat{E} - 2ik_y k_x s_{xy}\hat{E} - k_y^2 s_{yy}\hat{E}\right)\right) exp[i(\omega t - k_y y)] + *$$

which can be rewritten to:

$$\hat{\eta}_b\left(\frac{\omega^2}{k^2} - gd\right) = \frac{1}{\rho}\left(\frac{{k_x}^2}{k^2}s_{xx}\hat{E} + \frac{k_x k_y}{k^2}s_{xy}\hat{E} + \frac{{k_y}^2}{k^2}s_{yy}\hat{E}\right) \tag{22}$$

where:

$$k = \sqrt{k_x^2 + k_y^2} \tag{23}$$

and:

$$\frac{{k_x}^2}{k^2} = \cos(\theta)^2, \frac{k_x k_y}{k^2} = \cos(\theta)\sin(\theta), \frac{{k_y}^2}{k^2} = \sin(\theta)^2 \tag{24}$$

where θ is the incidence angle of the bound long wave. With use of eqs. 19-21 we obtain the general expression for the bound long wave amplitude on a horizontal plane:

$$\hat{\eta}_b = \frac{\left(n(1 + cos(\alpha - \theta)^2) - \frac{1}{2}\right)\hat{E}}{\left(\frac{\omega^2}{k^2} - gd\right)} \tag{25}$$

In the case the two primary waves have the same direction the solution of Longuet-Higgins and Stewart (1964) is retained:

$$\hat{\eta}_b = \frac{\left(2n - \frac{1}{2}\right)\hat{E}}{\left(\frac{\omega^2}{k^2} - gd\right)} \tag{26}$$

3 Verification

To test the derivation and implementation we have compared the results to the analytical solutions provided by Shaffer [1990]. In this case the two primary waves have different frequencies but equal directions. The angular frequency of the primary waves, ω_1 and ω_2, are given by

$$\omega_1 = (1 - \epsilon)\omega_s, \omega_2 = (1 + \epsilon)\omega_s$$

where ω_s is the mean angular frequency of the primary waves and $\epsilon = 0.1$. The wave breaking parameters are $\gamma = .64$, $\alpha_d = 1.0$ and $n = 5$. The modulation of the wave energy with respect to the mean short wave energy is given by:

$$\hat{E} = \rho g \delta a^2$$

where δ is taken to be 0.1 and the mean amplitude of the short waves, a, equals 0.0248 (m). The angle of incidence, α, ranges between 1^o and 60^o with respect to the coast normal using a plane beach with a slope m of 0.05 and an offshore depth, h_0 of 0.2485 m. Next we compare the normalised surface elevation amplitude at the shore line as function of the incidence angle to the analytical results (see the right panel of Figure 1). Where the normalized surface elevation amplitude is given by:

$$\frac{\hat{\eta}}{\delta a} \tag{27}$$

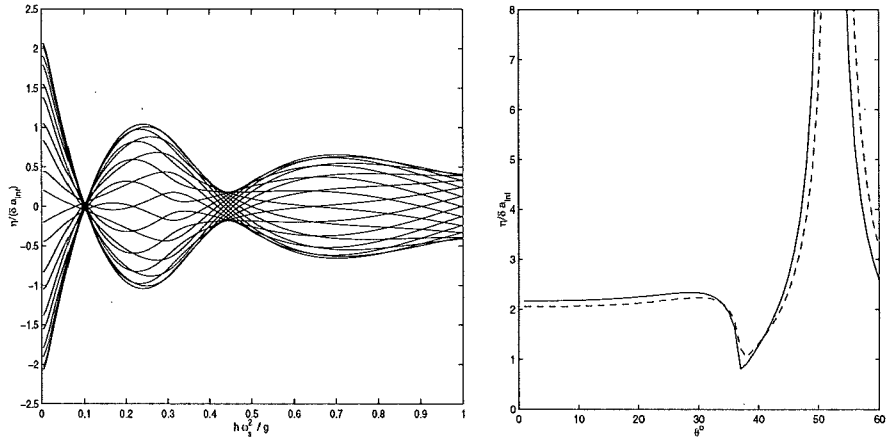

Figure 1: Left panel: Snapshots of computed surface elevation for $\alpha = 30°$. Right panel: Normalised long wave surface elevation amplitude at the shore line (solid line) compared to analytical solution given by Schäffer [1990] (dashed line).

Small differences occur, which can at least in part be ascribed to the alternative wave dissipation formulation. Overall the comparison shows good agreement. The fact that for $\alpha = 53^o$ the shore line elevation goes to infinity indicates the presence of resonant interaction between the short wave groups and the underlying long waves c.q. edge wave.
Next we consider two primary waves with different frequencies and directions:

$$\eta_1 = \hat{\eta}_1 sin(\omega t - k_1 cos(\alpha_1)x - k_1 sin(\alpha_1)y) \tag{28}$$

and

$$\eta_2 = \hat{\eta}_2 sin(\omega t - k_2 cos(\alpha_2) - k_2 sin(\alpha_2)y) \tag{29}$$

where the mean incidence angle of the short waves is given by:

$$\alpha = atan\left(\frac{k_1 sin(\alpha_1) + k_2 sin(\alpha_2)}{k_1 cos(\alpha_2) + k_2 cos(\alpha_2)}\right) \tag{30}$$

and the incidence angle of the energy modulation and bound long wave:

$$\theta = atan\left(\frac{k_1 sin(\alpha_1) - k_2 sin(\alpha_2)}{k_1 cos(\alpha_2) - k_2 cos(\alpha_2)}\right) \tag{31}$$

In this case the bound long wave behaviour changes considerably. Not only will the propagation direction of the bound long wave be different from the mean primary wave direction, also the amplitude will change. The bound low frequency energy density for a synthetic short wave spectrum (shown in the left panel of Figure 2) at a waterdepth of 3 m is computed with eq. 22 and compared to the non-linear solution for three-wave interaction given by Hasselmann (1962). The comparison is good.

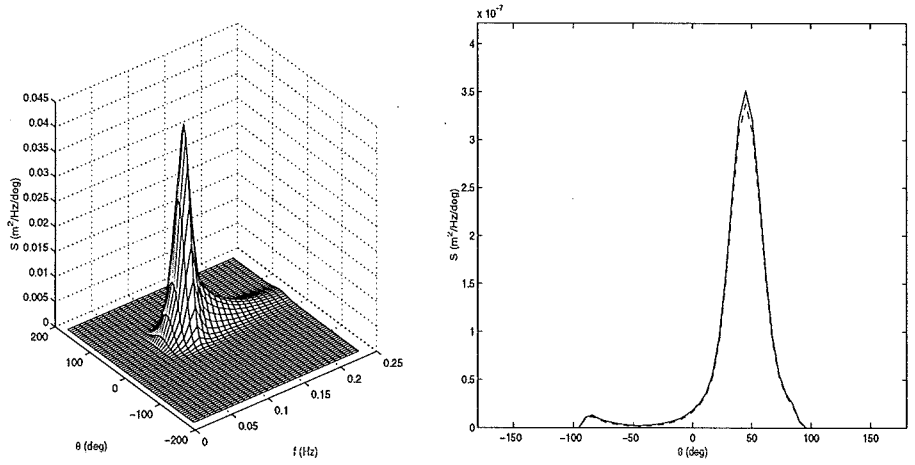

Figure 2: Left panel: Short wave energy density spectrum. Right panel: Comparison of corresponding bound low frequency energy density according to eq. 22 (solid line) and Hasselmann (1963) (dashed line)

4 Test case

4.1 Introduction

The behaviour of the model is assessed with a realistic testcase: the generation of low frequency energy by obliquely incident short waves during the DELILAH field experiment. The DELILAH experiment was performed in 1990 at the US Army Corps of Engineers Field Research Facility at Duck, North Carolina. The positions of colocated velocity meters and pressure transducers are shown in Figure 3. A cross-shore array was deployed to measure the wave transformation and cross-shore distribution of the longshore current velocities.

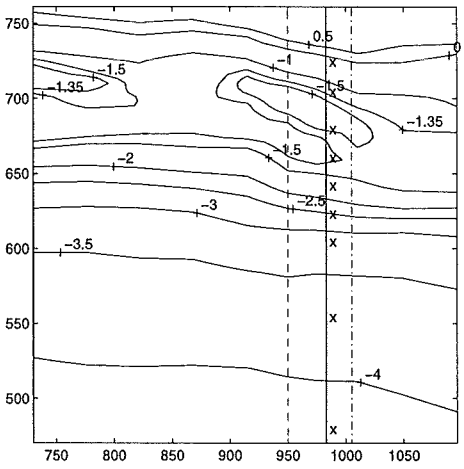

Figure 3: Bathymetry for Oct 10 and position of instruments in cross-shore array

The input short wave spectrum is obtained by a maximum entropy frequency-directional analysis of the puv-signals (pressure, cross-shore and alongshore velocities) at the measuring point furthest offshore in the cross-shore array. The resulting short wave spectrum for Oct10 from 10h-11h is shown in the upper panel of Figure 4.

The significant wave height at that time was 1.0 m with a mean direction of aproximately -25 deg with the shore normal and a peak frequency of .9 Hz. The measured bound long wave energy, shown in the lower panels of Figure 4, is estimated with a bispectral analysis (Hasselmann et al., 1963).

4.2 Long wave computation

The offshore boundary condition for the low frequency computations is set at 8 m water depth. To this end the spectrum, shown in the upper panel of Figure 4, is inversely shoaled and refracted towards this water depth, to account for the generation of free long waves while propagating from 8 m towards the first offshore measuring point. Beyond this water depth the generation of free long waves is expected to be negligible. The computed low frequency energy density for the present test case is shown in Figure 5.

The comparison with the bound low frequency energy density, compare with lower panels of Figure 4, is favourable for the offshore locations. Further inshore the comparison is less good. We mention the fact that the computed bound long wave energy density is based on the assumption that forcing and the bound long waves are in equilibrium (like on a horizontal plane). This is more or less the case at deeper water but no so as the waterdepth becomes small with respect to the short wave height. However, in that case one would expect that the bound long wave is overpredicted and not underpredicted as is the case here. The latter is most likely associated with the fact that in the computations the modulation of the short wave energy disappears as the waves start breaking whereas in reality this is not the case. As for the total energy density the comparison is less good. Though the nodal features seem

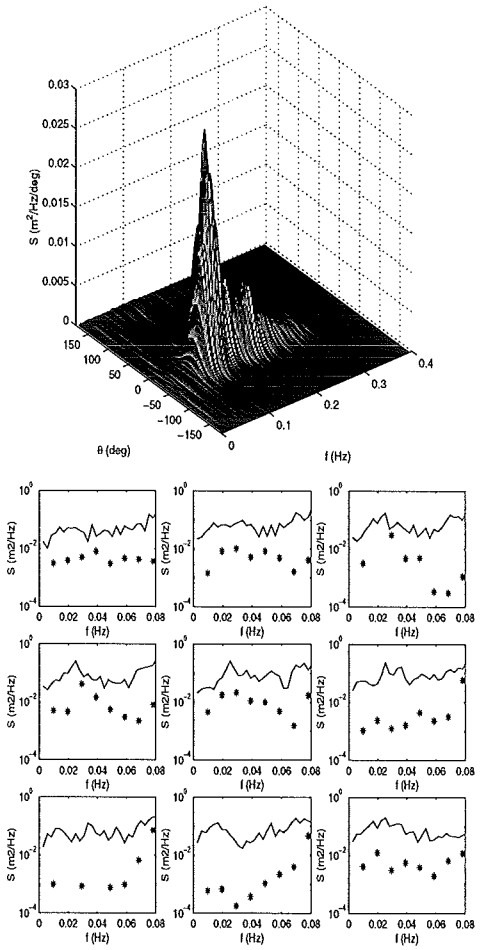

Figure 4: Upper panel: Short wave energy density spectrum for Oct10, 10h-11h. Lower panel: Total (solid line) and bound (asterisks) low frequency energy density at measurement locations starting offshore (upper left) towards the shore (lower right

to be reproduced in some sense, the intensity is a factor 10 too small. This can be related to a number of phenomena such as the set-up, longshore current and short wave modulation within the surfzone. These effects will be investigated further.

The computed directional spreading is shown in Figure 6 (same sequence as in previous figures). The bound low frequency energy density is shown in the upper panels. The energy density is restricted to a relatively narrow area which is governed by the directional spreading of the short waves. The short wave breaking strongly decreases the bound low frequency energy density.

More intriguing is the observed pattern in the total low frequency energy density (lower panels of Figure 6), which shows areas of low energy density alternated by areas of high energy density associated with standing wave patterns. It is also clear that the directional spreading in this case is much broader than in the case of bound low-frequency energy density only. This is related to the fact that the free long

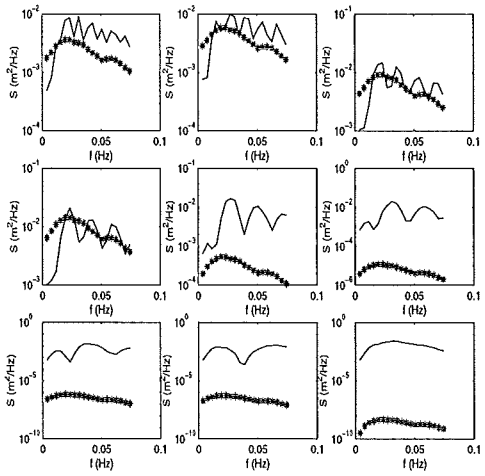

Figure 5: Computed total (solid) and bound (asterisks) low frequency energy density spectrum for Oct10 10h-11h

waves are refracting much stronger than the bound long waves. This has important consequences for the long wave decay in the offshore direction as observed by Herbers et al. [1990].

5 Conclusions

A linear model to examine the generation of surfbeat forced by directionally spread wind waves has been developed. A first assessment of the directional characteristics of the surfbeat clearly shows the differences between bound long waves and free long waves. An improved comparison with data nessecitates a closer look at the effects of wave breaking, set-up, longshore currents and bottom friction.

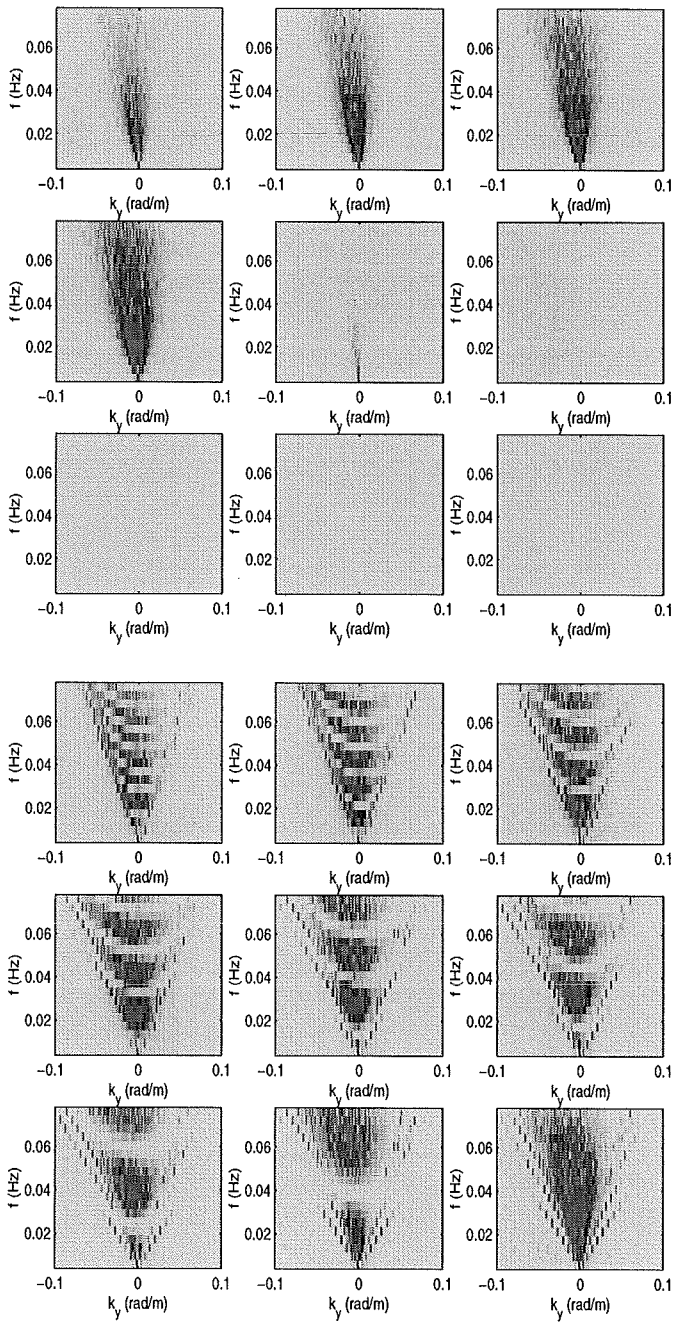

Figure 6: Upper nine panels: Directional spreading of bound low frequency energy density Oct10, 10h-11h. Lower nine panel: Directional spreading of total low frequency energy density.

Acknowledgements

The present progress report results from a collaboration with the Naval Postgraduate School which enabled us to use the time series in the test case. Additional data were provided by the Field Research Facility of the U.S. Army Engineer Waterways Experiment Station's Coastal Engineering Research Center. Permission to use these data is appreciated. The sponsoring by the National Institute for Coastal and Marine Management (RIKZ) through the Netherlands Centre for Coastal Research (NCK) is also greatly appreciated.

References

Birkemeier, W.A., 1991: DELILAH nearshore processes experiment: Data summary, miscellaneous reports, Coastal Eng. Res. Cent., Field Res. Facil., U. S. Army Eng. Waterw. Exp. Sta., Vicksburg, Miss..

Hasselmann, K., 1962: On the non-linear energy transfer in a gravity-wave spectrum. Part I: General theory. JFM, 12, pp. 481-500.

Herbers, T.H.C., S. Elgar and R.T. Guza, 1994: Infragravity-frequency (0.005 - 0.05 Hz) motions on the shelf. Part 1: Forced waves. JPO, 24, pp. 917-927.

Herbers, T.H.C., S. Elgar, R.T. Guza and W.C. O'Reilly, 1992: Infragravity-frequency (0.005-0.05 Hz) motions on the shelf. Proc. 23 ICCE, ASCE, Venice.
Longuet-Higginns, M.S. and R.W. Stewart, 1964: Radiation stresses in water waves: a physical discussion, with applications. Deep-sea Res. 11, pp. 529-562.

Roelvink, J.A., 1993: Dissipation in random wave groups incident on a beach. J. of Coastal Eng., vol 19, pp. 127-150.

Schäffer, H.A., 1990: Infragravity water waves induced by short wave groups. PhD thesis, Institute of hydrodynamics and hydraulic engineering, Technical University of Denmark, series paper No. 50.

Symonds G., D.A. Huntley and A.J. Bowen, 1982: Two-dimensional surfbeat: long wave generation by a time varying breakpoint. JGR, 87, No. C1, pp. 492-498.